# New Island of $\mu$s Isomers in Neutron-Rich Nuclei around the $Z = 28$ and $N = 40$ Shell Closures

R. Grzywacz,[1,2,3] R. Béraud,[4] C. Borcea,[5] A. Emsallem,[4] M. Glogowski,[1] H. Grawe,[6] D. Guillemaud-Mueller,[7] M. Hjorth-Jensen,[8] M. Houry,[4] M. Lewitowicz,[3] A. C. Mueller,[7] A. Nowak,[1] A. Płochocki,[1] M. Pfützner,[1,6] K. Rykaczewski,[1,9,10] M. G. Saint-Laurent,[2] J. E. Sauvestre,[11] M. Schaefer,[12] O. Sorlin,[7] J. Szerypo,[1] W. Trinder,[2] S. Viteritti,[4] and J. Winfield[4]

[1]*IFD, Warsaw University, Pl-00681 Warsaw, Hoża 69, Poland*
[2]*GANIL, B.P. 5027, 14021 Caen Cedex, France*
[3]*University of Tennessee, Knoxville, Tennessee 37996*
[4]*IPN Lyon, 69622 Villeurbane Cedex, France*
[5]*IAP, P.O. Box MG6, Bucharest-Magurele, Rumania*
[6]*GSI, Postfach 110552, D-64220, Darmstadt, Germany*
[7]*IPN, IN2P3-CNRS, 91406, Orsay Cedex, France*
[8]*Nordita, Blegdamsvej 17, DK-2100 Copenhagen, Denmark*
[9]*Physics Division, ORNL, Oak Ridge, Tennessee 37830*
[10]*IKS, Leuven, B-3001, Leuven, Belgium*
[11]*CE Bruyères-le-Châtel, B.P. 12, F-91680 Bruyères-le-Châtel, France*
[12]*University of Göttingen, D-37073, Göttingen, Germany*

(Received 22 January 1998)

New isomeric states in the neutron-rich nuclei near the $Z = 28$ and $N = 40$ shell closures have been identified among the reaction products of a $60.3A$ MeV $^{86}$Kr beam on a $^{\mathrm{nat}}$Ni target. From the measured isomeric decay properties information about the excited states and their nuclear structure has been obtained. The isomerism is related mostly to the occupation of the neutron $g_{9/2}$ orbital, an intruder level in the $N = 3$ $fp$ shell. It is illustrated with the decay properties of $^{69}$Ni$^m$, $^{70}$Ni$^m$, and $^{71}$Cu$^m$ interpreted within the nuclear shell model. [S0031-9007(98)06719-2]

PACS numbers: 25.70.Mn, 21.10.Tg, 23.20.Lv, 27.50.+e

The regular appearance of the nuclear isomers in the vicinity of closed shells was one of the first phenomena naturally explained by the nuclear shell model. It contributed much to the understanding of the nuclear structure in the early stage of the shell-model formulation [1], pointing out the existence of the spin-orbit term. In a standard shell-model description isomeric decay properties allow one to draw conclusions on the evolution of single particle states as well as on the residual interactions between valence nucleons [2].

For nuclei with very large neutron excess dramatic changes in the shell structure such as disappearance of the shell gap [3] and appearance of new shell closures are predicted, which are intimately related to the small neutron binding energy. The basic difficulty to access these nuclei by standard nuclear reactions, even with radioactive ion beams, is relieved in a twofold way by isomer spectroscopy following high-energy fragmentation and fission with full in-flight identification. The unprecedented selectivity of the method allows extraction of nuclear structure information at a production level of $\leq 1$ atom/s [4], and the excitation energy of the isomer, if close enough to the neutron separation energy, simulates ground states of even more exotic nuclei, yet inaccessible. Beyond the aspect of nuclear structure in neutron-rich nuclear matter and/or at low nuclear density, the experimental data are of key importance for the understanding of the astrophysical $r$-process [5,6].

In this paper we present the new spectroscopic data obtained for nuclei near shell closures at $Z = 28$ and $N = 40$. The existence of the $N = 40$ subshell closure was suggested experimentally by Broda *et al.* [8] for the $^{68}_{28}$Ni$_{40}$ nucleus. The strength of this subshell closure and its persistence for $Z < 28$, which is questionable according to shell model calculations [7], determine the waiting point for the astrophysical $r$-process at $^{64}_{24}$Cr$_{40}$ [6].

In a pioneering experiment [4], the known proton-rich "island of isomers" with $N \approx 50$, $40 < Z < 50$ was investigated. The isomerism in this region is due to the occupation of the proton $\pi g_{9/2}$ orbital, forming *seniority isomers* in stretched $\pi g^n_{9/2}$ configurations, and *single particle isomers* due to the large spin difference to the neighboring $\pi p_{1/2}$ orbital. This gives rise to the $8^+$ $E2$ isomers in the $N = 50$ isotones $^{92}$Mo, $^{94}$Ru, $^{96}$Pd, and $^{98}$Cd, and the long known $\pi p_{1/2}$-$\pi g_{9/2}$ $M4$ isomerism. The neutron-rich nuclei studied in this work with $Z \approx 28$, $40 < N < 50$, are the "valence mirrors" (to the $N = 50$, $40 < Z < 50$ region) with the role of protons and neutrons outside the closed shell interchanged. The close lying neutron $\nu f_{5/2}$ orbital strongly interacting with its spin-orbit partner $\pi f_{7/2}$ takes the part of the $\nu g_{9/2}$ counterpart with a large spin-parity difference, giving rise to well known $M2$ isomers in proton-rich $N > 28$ nuclei like $^{67}$Zn, $^{67}$Ge, $^{69}$Ge, or $^{71}$Se. To date information about excited states in the region of the neutron-rich isotopes in the vicinity of the magic $Z = 28$ number is very scarce. Previous to the present experiment data about excited states for the nickel isotopes were obtained using multinucleon transfer reactions [8,9]. In latter studies, a $5^-$ isomer in $^{68}$Ni and a $9/2^+$ isomer in $^{67}$Ni were discovered. Observed isomers in $^{61}$Fe, $^{67}$Ni, and $^{69}$Cu were presented in [10] and earlier references therein. As is further shown, these isomers belong to the larger group of metastable states in the region concentrated around $N = 40$ and $Z = 28$.

The experiment was performed at GANIL Laboratory, using the SISSI production target device coupled to the system of the Alpha and LISE3 spectrometers with the same technique as described in Refs. [4,11]. The $n$-rich $^{86}$Kr$^{34+}$ isotope, with an energy of 60.3$A$ MeV and an intensity of 15 pnA on average, impinged on a rotating $^{\rm nat}$Ni target 100 $\mu$m thick placed inside SISSI. The heavy-ion detection system consisted of six planar silicon detectors (300, 300, 300, 500, 500, and 500 $\mu$m). The last four were placed at the final focus and were surrounded by five high-purity germanium detectors (HPGe) of about 70% efficiency each: four in a cross geometry and the fifth—a low energy photon spectrometer (LEPS)—was positioned behind the 1 mm thick back plate covering the implantation detectors. The sensitivity range for the $\gamma$-ray energies was between 40 and 4000 keV. Absolute efficiency of the system amounted to 12% for a sum of HPGe plus 4% for LEPS in maximum at 130 keV, and about 5% (all HPGe) for 1 MeV photons. The time of flight (TOF), referred to the cyclotron radio frequency, was measured between the target and the first telescope detector. The flight path was 118 m, which corresponded to typical TOF values of about 1.2 $\mu$s. Time elapsing between implantation and isomeric decay was measured up to 72 $\mu$s and was recorded using standard time-to-amplitude converter (TAC) modules. TAC's with 100 $\mu$s range were used for each individual detector. This allowed us to define $\gamma\gamma$ coincidences. The identification of mass ($A$), atomic number ($Z$), and ionic charge ($q$) of each detected heavy ion (HI) was done with the standard TOF–$\Delta E$-$E$ technique [12]. As a result, the HI-identification plot is obtained. The separation in mass-to-charge ratio ($A/q$) was sufficient to separate neighboring charge states of the same nuclide. The $\gamma$-gated identification plot, obtained in a way described in [4,11], reveals several isomers in the region; see Fig. 1 and Table I. The particle identification was confirmed by $^{67}$Ni$^m$ and $^{68}$Ni$^m$, identified by their known $\gamma$ radiation.

Thirteen new isomeric states were identified; see Fig. 1. The $\gamma$-ray spectra and their tentative decay patterns were determined for each observed case. A summary of the deduced data on excitation energy, half-life of the studied isomers together with proposed spin and parity assignments, energy and multipolarity for the isomeric transition is presented in Table I. The latter was based on the comparison of the measured half-life of the isomer with Weisskopf estimates for given transition energy. Only the cases where the isomeric decays were observed unambiguously are presented. A criterion was applied that at least five counts are seen in a single $\gamma$ line above the background in at least

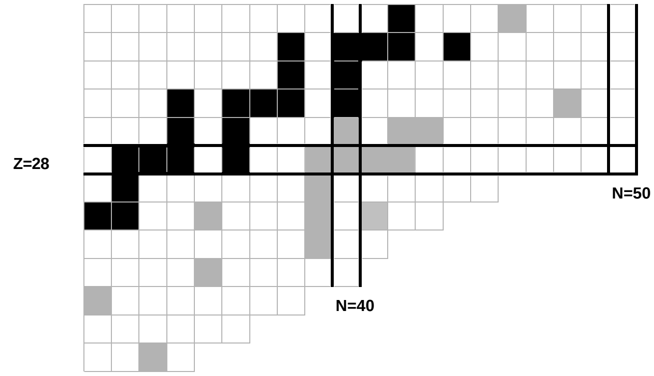


FIG. 1. Part of the chart of nuclei with the observed isomers (grey squares) and the stable nuclei (black squares). Magic numbers $Z = 28$ and $N = 40$ and 50 are given for orientation.

TABLE I. List of isomers observed with $^{86}$Kr beam. Given are $E^*$: deduced excitation energy, $T_{1/2}$: half-life, $I^\pi$: tentative spin of isomer, Mult.: multipolarity of the isomeric transition, $E_i^\gamma$: energies of the observed $\gamma$ lines. All isomers except $^{69}$Cu$^m$, $^{68}$Ni$^{m1,m2}$, $^{67}$Ni$^m$, and $^{61}$Fe$^m$ are observed for the first time in this work. For the cases marked with (*) only the strongest $\gamma$ lines are given, for others, all observed. Assumed isomeric transitions are printed in bold.

| | $E^*$ (keV) | $T_{1/2}$ ($\mu$s) | $I^\pi$ | Mult. | $E_i^\gamma$ (keV) |
|---|---|---|---|---|---|
| $^{54}$Sc$^m$ | 110 | 7(5) | $(5^+)$ | $E2$ | **110** |
| $^{54}$V$^m$ | 108 | 0.9(5) | $(5^+)$ | $E2$ | **108** |
| $^{59}$Cr$^m$ | 503 | 96(20) | $(9/2^+)$ | $M2$ | **208**,193<br>102 |
| $^{61}$Fe$^m$ | 861 | 0.25(1) | $(9/2^+)$ | $M2$ | **654**,207 |
| $^{64}$Mn$^m$ | 135 | >100 | | $M2$ | **135** |
| $^{65}$Fe$^m$ | 364 | 0.43(13) | $(5/2^-)$ | $M2, E2$ | **364** |
| $^{66}$Co$^{m1}$ | 175 | 1.21(1) | $(5^+)$ | $E2$ | **175** |
| $^{66}$Co$^{m2}$ | 642 | >100 | $(8^-)$ | $M2$ | **252**,214<br>175 |
| $^{67}$Fe$^m$ | 367 | 43(30) | $(5/2^-)$ | $M2$ | **367** |
| $^{67}$Ni$^m$ | 1007 | 13.3(2) | $9/2^+$ | $M2$ | **313**,694 |
| $^{68}$Ni$^{m1}$ | 2847 | 860(50) | $(5^-)$ | $E3$ | **814**,2033 |
| $^{68}$Ni$^{m2}$ | 1770 | 0.34(3) | $0^+$ | $E0$ | 511 |
| $^{69}$Cu$^m$(*) | 2740 | 0.36(5) | $(13/2^+)$ | $E2, M1$ | **75,190**<br>680,1871 |
| $^{69}$Ni$^m$(*) | 2701 | 0.439(3) | $(17/2^-)$ | $E2$ | **148**,593<br>1959 |
| $^{70}$Ni$^m$ | 2860 | 0.21(5) | $(8^+)$ | $E2$ | **183**,448<br>970,1259 |
| $^{71}$Cu$^m$(*) | 2756 | 0.275(14) | $(19/2^-)$ | $E2$ | **133**,494<br>939,1189 |
| $^{72}$Cu$^m$ | 270 | 1.76(3) | $(4^-)$ | $E2$ | **51**,82<br>138 |
| $^{78}$Zn$^m$ | >1070 | >30 | | | 1070 |
| $^{79}$As$^m$ | 773 | 1.21(1) | $9/2^+$ | $M2$ | **542**,231 |

two different $\gamma$ detectors and both decay with a similar lifetime range. An evidence for several other, more exotic isomers was obtained which, however, do not fulfill this rather stringent criterion. The proposed spin-parity assignments to the new isomers, unless otherwise stated below, are based on the systematics of states with assigned configurations, of quasiparticle energies in the region $Z \leq 28$, $N \geq 28$, and on the valence mirror concept for the Ni isotopes.

As shown in Fig. 1 there is a group of isomers along the $Z = 28$ and $N = 39$ lines. The $N = 39$, $Z = 25-28$ isomers have much shorter lifetimes than their counterparts in the valence mirror region $Z = 39$, $N \leq 50$. Comparing the measured half-lives and transition energies with those given by Weisskopf estimates one can safely assign the $M2$-type for the isomeric transitions. This requires a change of parity between the involved states. In case of $^{67}Ni^m$ we have measured a half-life of $13.3 \pm 0.2$ $\mu$s, which allows one to determine $B(M2) = 0.047$ W.u. for this transition. This completes the interpretation of $^{67}Ni^m$ (see [9,10]) as a $\nu g_{9/2}$ state decaying to the $(\nu f_{5/2})^{-1}$ level via the $M2$ transition. This isomeric transition is followed by an $E2$ decay to the ground state, having a $\nu p_{1/2}$ configuration. The $M2$ interpretation of the isomeric 363.5 keV transition in $^{65}Fe^m$ suggests the same orbitals involved; however, the systematics of $\nu g_{9/2}$ and $f_{5/2}$ quasiparticle energies in Ni, Fe, and Cr isotopes [13] favor reversed level order, i.e., an $I^\pi = 5/2^-$ assignment to the isomer as in $^{67}Fe^m$. This is in agreement with the $\nu h_{11/2}$-$g_{7/2}$ systematics in $Z \leq 50$ nuclei one major shell higher [13]. For the odd-odd isotopes ($Z = 27, 25$), the possible spins of $M2$ isomers are ranging from $6^+$ to $8^-$ due to the coupling of $f_{7/2}$ proton holes to $f_{5/2}$ neutron holes and to $g_{9/2}$ neutron particles. Spin-parity assignments are difficult due to missing ground state assignments, which is only available for $^{66}Co$. For odd and even mass $N = 39$ isotones we observe a large decrease of the isomer excitation energy from 1007 to 503 keV with decreasing $Z$. This can be explained by the proton-neutron interaction in the open $\pi f_{7/2}$ shell as in the corresponding $Z \leq 50$ nuclei one major shell higher without invoking deformation at the present status of experimental evidence.

The concept of valence mirror nuclei gives a consistent picture for the nickel isotopes, where the new isomers $^{69}Ni^{m1,m2}$ and $^{70}Ni^m$ were observed. For the case of $^{69}Ni$, the relatively high production rate allowed for the identification of several levels and for subsequent analysis of their coincidence relations. The proposed decay scheme is shown in Fig. 2. Note that the proper reconstruction of the $^{69}Ni^m$ decay scheme requires that the 594 keV line is a doublet, which was confirmed by the $\gamma\gamma$ coincidence analysis. The analysis of relative transition intensities and coincidence relations led to the location of two isomeric states, with a short lived one at $E^* = 2701$ keV excitation and half-life of $T_{1/2} = 0.439(3)$ $\mu$s. The suggested second isomer is a long lived, low lying ($E^* = 321$ keV) state with $I^\pi = 1/2^-$ and is most probably $\beta$ decaying. The estimated half-life of $\beta$ decay of this isomer amounts to about 3 sec if the experimental $\log(ft) = 4.7$ value determined for the Gamow-Teller decay of $^{67}Ni$ [14] is assumed. The $\beta$ decay of this isomer should populate the $3/2^-$ ground state of $^{69}Cu$. The Weisskopf estimate for the half-life for the 321 keV $M4$ transitions is 14 days and $\gamma$ deexcitation of this isomer is not to be observed. The valence partner of this nucleus is $^{91}Nb$, where two similar isomers ($^{91}Nb^{m1}$, $E^* = 2034.4$ keV, $I^\pi = 17/2^-$, $T_{1/2} = 3.76$ $\mu$s, and $^{91}Nb^{m2}$, $E^* = 104.5$ keV, $I^\pi = 1/2^-$, $T_{1/2} = 60.86$ $d$ [13]) were identified. This supports the interpretation of $^{69}Ni^{m1,m2}$. The position of the low lying isomer fixes the single particle energy of the $\nu p_{1/2}$ relative to $\nu g_{9/2}$ orbital.

Important nuclear structure information is related to the decay of $^{70}Ni^m$ (Fig. 2). It has a half-life of 210(50) ns, much shorter than the TOF value. This isomer can be assigned to the predicted group of $8^+$ *seniority isomers* in $^{70,72,74,76}Ni$ which have proton valence partners ($8^+$ isomers in $N = 50$ $^{92}Mo$, $^{94}Ru$, $^{96}Pd$, and $^{98}Cd$ [11,15]). The spin of the $8^+$ isomer is the maximum one for the configuration of $(g_{9/2})^2$ for identical particles. The isomer deexcitation occurs via four consecutive $E2$ transitions connecting $8^+$, $6^+$, $4^+$, $2^+$, and $0^+$ states. The observation of $^{70}Ni^m$ gives not only the energy 1259 keV of the $2^+$ state, but also the strength of the $(\nu g_{9/2})^2$ interaction, which can be compared to those of protons [2]. The lower energy 1259 keV of $2^+$ state in $^{70}_{28}Ni_{42}$ as compared to 2033 keV observed for $^{68}_{28}Ni_{40}$ is an important fact confirming the subshell closure at $N = 40$ for nickel isotopes.

At $N \approx 50$, on the proton-rich side, protons and neutrons occupy the same $g_{9/2}$ orbital and the strong proton-neutron interaction manifests itself as is illustrated by the $14^+$ isomer in $^{94}Pd$ [16]. On the contrary, for the very neutron-rich nuclei the valence nucleons belong to different major shells, and proton-neutron interaction is expected to play a minor role at low excitation energies. One may illustrate this with the observed properties of the $^{71}Cu^m$ isomer. The strongest $\gamma$ transitions detected in the deexcitation of the $^{71}Cu^m$ isomer have very similar energies to those of the $^{70}Ni^m$ decay; see Fig. 2. We interpret this as decay of a $19/2^-$ isomer which has the $(\nu g_{9/2})^2_{I=8^+} \times \pi p_{3/2}$ configuration. The $E2$ cascade follows the level sequence $15/2^-$, $11/2^-$, $7/2^-$, and $3/2^-$ where the $p_{3/2}$ proton wave function is coupled to the $6^+$, $4^+$, $2^+$, and $0^+$ states, respectively. The proton-neutron interaction between the nucleons $\pi p_{3/2}$ and $\nu g_{9/2}$ is in this case too weak to influence the strongly coupled $(\nu g_{9/2})^2$ pair. Both $^{71}Cu^m$ and $^{70}Ni^m$ are good examples of the pure $\nu\nu$ interaction of a valence neutron pair.

For $^{69,70}Ni$ we compare our experimental data to the respective spectra of excited states predicted by a shell-model calculation using a $G$ matrix residual interaction. The interaction was derived for a $^{56}Ni$ core following

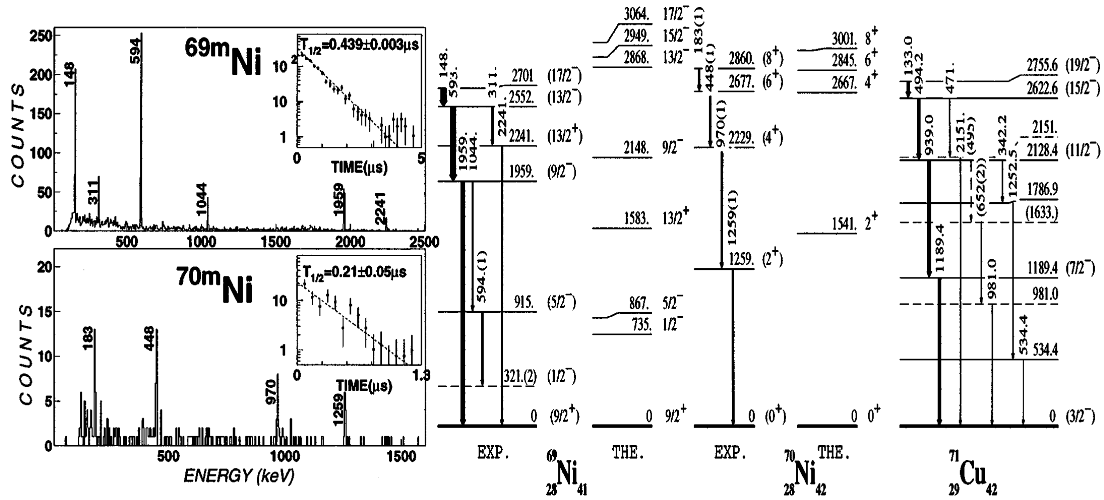


FIG. 2. Observed $\gamma$ spectra of $^{69}\mathrm{Ni}^{m}$ and $^{70}\mathrm{Ni}^{m}$. For both cases, decay schemes deduced from the data (EXP.) and predicted by the shell model (THE.) are also presented. The time decay patterns (in the insets) were obtained taking the strongest observed gamma transitions. The decay scheme of $^{71}\mathrm{Cu}^{m}$ with its main decay sequence resembling that of $^{70}\mathrm{Ni}^{m}$ is also presented. All energies are given in keV.

the method outlined by Hjorth-Jensen *et al.* [17,18]. Experimental neutron single particle energies from $^{57}$Ni for the active orbitals $p_{3/2}$ (0.0 MeV), $f_{5/2}$ (0.77 MeV), $p_{1/2}$ (1.11 MeV), and $g_{9/2}$ (3.70 MeV) were used in the shell-model calculation. The presented results as well as those obtained with previously derived realistic interactions [2,19] obviously fail to reproduce the relative positions of odd and even parity states, which may be due to the deficiency of realistic interactions in accounting for the monopole part of the interaction [7,20]. The $B(E2)$ values calculated for the isomeric transitions in $^{69,70}$Ni, $B(E2;17/2^- \rightarrow 13/2^-) = 21.5\ e^2\,\mathrm{fm}^4$ and $B(E2;8^+ \rightarrow 6^+) = 6.26\ e^2\,\mathrm{fm}^4$, deviate from the experimental values 15.8(1) and 12(3) $e^2\,\mathrm{fm}^4$ in opposite directions, which points to a deficiency in the wave functions rather than in the effective operator. The shell-model $B(E2)$ values have been obtained using an effective neutron charge $e_n = 1$. As was shown by Grawe *et al.* [2], one can fit locally the shell-model parameters to reproduce the experimental spectra for $^{69}$Ni and $^{70}$Ni, but the predictive power of this approach should be verified with further experimental studies of more neutron-rich isotopes, including complementary beta-decay measurements; see [21].

In conclusion, the experimental data led to the observation of a new isomeric island. Decay properties of thirteen new isomers have been found. The proposed interpretation of the structure of the Ni isomeric states is based on the valence mirror concept, which is particularly transparent for $^{70}\mathrm{Ni}^{m}$, proving the similarity of the $\pi\pi$ and $\nu\nu$ interaction. We found a series of isomers originating from the coupling of $g_{9/2}$ neutrons. This allows one to deduce the $(\nu g_{9/2})^2$ effective interaction for the very neutron-rich nickel isotopes [2].

The method of the microsecond correlation between implanted heavy ions and $\gamma$ radiation applied to fragmentation reactions is a very efficient spectroscopic tool. Its capability for simultaneous measurement of many nuclear species allows for the investigation of nuclear structure effects in a systematic way. The increase of $\gamma$ efficiency due to the use of existing cluster and clover detectors can compensate for the decrease of the production cross section for the most $n$-rich fragments. With this method, in the region of neutron-rich nickel isotopes, further experimental progress is feasible.

Support by IN2P3 and by the KBN is acknowledged.

[1] A. de Shalit and H. Feshbach, *Theoretical Nuclear Physics,* Nuclear Structure Vol. 1 (Wiley, New York, 1990).
[2] H. Grawe *et al.,* Prog. Part. Nucl. Phys. **38**, 15 (1997).
[3] J. Dobaczewski *et al.,* Phys. Rev. Lett. **72**, 981 (1994).
[4] R. Grzywacz *et al.,* Phys. Lett. B **355**, 439 (1995).
[5] F.K. Thielemann *et al.,* Nucl. Phys. **A570**, 329c (1994).
[6] O. Sorlin *et al.,* Nucl. Phys. A (to be published).
[7] A. Poves (private communication).
[8] R. Broda *et al.,* Phys. Rev. Lett. **74**, 868 (1995).
[9] T. Pawłat *et al.,* Nucl. Phys. **A574**, 623 (1994).
[10] R. Broda *et al.,* in *Proceedings of the International Conference on Fission and Properties of Neutron-Rich Nuclei,* edited by J.H. Hamilton and A.V. Ramayya (World Scientific, Singapore, 1998).
[11] R. Grzywacz *et al.,* Phys. Rev. C **55**, 1126 (1997).
[12] D. Bazin *et al.,* Nucl. Phys. **A515**, 349 (1990).
[13] Data Base, National Nuclear Data Network, Brookhaven.
[14] E. Runte *et al.,* Nucl. Phys. **A441**, 237 (1985).
[15] M. Górska *et al.,* Phys. Rev. Lett. **79**, 2415 (1997).
[16] M. Górska *et al.,* Z. Phys. A **353**, 233 (1995).
[17] M. Hjorth-Jensen, T.T.S. Kuo, and E. Osnes, Phys. Rep. **261**, 125 (1995).
[18] M. Hjorth-Jensen *et al.* (to be published).
[19] J. Sinatkas *et al.,* J. Phys. G **18**, 14 013 (1992).
[20] A. Abzouzi *et al.,* Phys. Rev. Lett. **66**, 1134 (1991).
[21] S. Franchoo *et al.* Phys. Rev. Lett. (to be published).